Environment International, Vol. 8, pp. 45-57, 1982
Printed in the USA.

0160-4120/82/070045-13$03.00/0

INDOOR RADON SOURCE FLUXES: EXPERIMENTAL TESTS OF A TWO-CHAMBER MODEL

Thomas L. Hernandez*
Center for Energy and Environmental Studies, Princeton University, Princeton, NJ 08544, USA

James W. Ring
Department of Physics, Hamilton College, Clinton, NY 13323, USA

Modeling houses as two coupled chambers, namely, the living area and basement, predicts more accurately the total indoor radon source flux from building materials and geology than a one-chamber model in houses with disparate radon concentrations. Three regional surveys found mean radon concentration ratios between basement and living area to range from 1.4 to 4.2, implying weak interchamber coupling in most cases. The invariability of second-order system parameters under steady infiltration but different initial conditions confirms the adequacy of the two-chamber model. The presence of a characteristic radon source flux was detected within the basements of two houses, in one case across different infiltration, coupling, and initial conditions. One-chamber models fit to two-chamber tracer gas data in one house show a source flux variation of a factor of 6 across changing coupling, while the two-chamber source flux variation was only a factor of 1.5. A substantial fraction of the apparent one-chamber living area source flux in these cases is the variable convective radon flux from the basement. The technique is not sensitive enough to detect living area source fluxes if either the interchamber coupling is strong or if the basement source flux is substantially larger.

Introduction

Knowledge of the total indoor radon source flux in residences is an important goal of the expanding field of building science. It would assist proposed field surveys in search of radon-problem regions of the country (Sachs *et al.*, 1982). An accurate estimate of both source flux and indoor location would assist mitigation measures in problem houses.

This paper presents an improved technique for determining the indoor radon source flux from both the living area and basement of a house. By modeling a house as two chambers, each perfectly mixed, a multichamber tracer gas injection technique described by Sinden (1978) is used to determine infiltration and interchamber volume flows. Indoor radon source fluxes are calculated from a steady radon flux balance applied around each chamber.

The magnitude of indoor source fluxes has typically been estimated by modeling a residence as a single, perfectly mixed chamber without specifically accounting for the basement volume or assuring good mixing between living area and basement. If the convective interchamber coupling is unsteady, the one-chamber model can give widely varying source flux results. Using this model, the actual source flux may be underestimated dramatically if it is assumed that the living area is convectively decoupled from the basement.

If applied around the living area, the one-chamber model accurately measures the total radon entering the living area, but the two-chamber model measures the actual amount of radon entering a residence from building materials and geology. In identifying a regional radon problem, it eliminates an additional variable parameter, interchamber coupling, which convectively transports radon between chambers. The two-chamber model easily takes variable interchamber coupling into account.

Coupling Ratio and Interchamber Coupling

Table 1 shows a sample of the radon concentrations in the living area and basement taken from homes in

*Present address: ECRI, 5200 Butler Pike, Plymouth Meeting, PA 19462.

Table 1. Radon concentration summary in the living area and basement for three regional surveys.

New York–New Jersey Radon Concentrations [pCi/1][a] Source: George and Breslin, 1980			Eastern Pennsylvania Radon Concentrations [pCi/1][b]					Princeton, NJ Radon Concentrations [pCi/1][c]		
				Winter 1981		Summer 1981			Winter–Spring 1981	
House #	LA	B	House #	LA	B	LA	B	House #	LA	B
1	2.6	3.6	1	13.1	4.1	2.0	7.9	1	1.1	15.0
2	1.3	4.4	2	75.0	29.4	1.8	20.5	2	1.7	11.5
3	2.0	4.1	3	30.5	22.1	31.7	69.6	3	1.5	9.0
4	3.1	3.4	4	1.1	1.0	0.4	0.4	4	11.0	25.0
5	1.3	2.2	5	3.7	6.7	1.6	5.2	5	7.4	14.0
6	–	1.2	6	17.1	37.4	2.0	25.9	6	2.3	7.0
7	1.0	1.4	7	29.2	28.2	11.4	52.8	7	0.6	1.8
8	1.0	2.1	8	13.3	25.9	6.5	–	8	0.2	1.9
9	0.5	2.3	9	1.2	5.2	1.5	1.5	9	0.2	1.2
10	1.1	2.8	10	8.7	16.8	2.2	13.3	10	0.2	1.1
11	0.3	–	11	6.2	18.9	2.9	6.9	11	1.0	1.0
12	0.3	–	12	19.0	24.6	6.8	17.8			
13	0.8	1.0	13	6.2	12.7	0.4	10.5			
14	0.6	1.5	14	1.9	1.5	1.2	2.2			
15	1.0	2.7	15	14.0	8.4	6.0	8.0			
16	0.5	0.7	16	3.5	4.8	6.0	11.7			
17	0.4	1.1	17	1.0	2.2	1.3	2.5			
18	0.5	0.9	18	2.6	1.0	0.8	1.1			
19	0.4	0.4	19	3.3	8.1	1.0	0.8			
20	0.4	1.0	20	1.4	2.8	0.5	0.6			
21	0.8	–	21	1.9	3.0	0.4	5.2			
			22	88.2	73.4	34.6	39.9			
			23	0.6	0.6	0.2	0.9			
			24	0.9	3.5	1.9	22.1			
			25	2.1	0.1	–	–			
			26	1.9	1.2	0.5	0.9			
			27	2.9	3.3	0.8	2.6			
			28	2.8	3.1	–	–			
			29	7.6	11.2	–	–			
			30	6.1	9.5	–	–			
			31	1.5	3.7	0.5	2.6			
			32	29.8	20.5	1.9	7.2			
			33	3.0	1.5	1.0	3.5			
			34	0.8	46.1	8.1	37.5			
			35	0.6	5.6	1.0	15.6			
			36	2.4	4.7	0.7	0.5			

[a]Mean 1-week time-integrated values over a 2-yr period.
[b]Integrated values.
[c]Integrated and instantaneous values.

New York and New Jersey (George and Breslin, 1980), eastern Pennsylvania, and Princeton, NJ. Concentrations were obtained using either instantaneous or integrated measurement techniques. Regardless of measurement type, the table shows that the basement and living area concentrations may be disparate by a factor of 10 or more.

For concentrations I_b and I_l in the basement and living area, the concentration ratio R_c is defined as

$$R_c = \frac{I_b}{I_l} . \quad (1)$$

Table 2 shows the mean concentration ratio for each region. Obviously, the two chambers cannot be considered well-mixed in most of the houses in these surveys.

The value of R_c can change dramatically as interchamber coupling changes, as is evident from the differ-

Table 2. Mean regional radon concentration ratios.

Region	Sample Size	R_c[a]	σ[b]
Princeton, NJ	11	4.2	2.2
E. Pennsylvania (summer)	31	3.2	2.5
E. Pennsylvania (winter)	36	1.4	3.0
New York–New Jersey	17	1.9	1.5

[a]Geometric mean radon concentration ratio where $R_c = I_b/I_l$ in a residence.
[b]Geometric standard deviation.

ences between the eastern Pennsylvania winter and summer data. For any residence with a basement, changing indoor temperature gradient may induce coupling changes by natural convection between seasons. In winter this produces the "stack effect," the net upward transport of warm, buoyant air, while in summer, a "negative stack effect," the downward flow of indoor air, may occur (ASHRAE, 1981). Coupling may change diurnally due to more modest diurnal changes in temperature gradient.

Much higher coupling, even infinite coupling (perfect interchamber mixing), may be induced by forced convection. If the heat distribution system uses forced air and the furnace is located in the basement, leaky basement ducts may permit a considerable amount of interchamber air exchange while the circulation fan is on. Because most furnaces are oversized (Bonne *et al.*, 1979), both R_c and coupling may change dramatically, with a period on the order of an hour, because the fan is on intermittently.

Radon Flux Density Variation

Both the radon flux density from the surface of a porous body J_s (in atoms or pCi/unit area/unit time) and the total indoor source flux S_j into chamber j (in atoms or pCi/unit time) are time-dependent functions of the rate of change of atmospheric pressure. For a particular porous medium, however, at constant conditions of soil permeability, J_s and S_j have mean or "characteristic" values which are independent of any condition of temperature and pressure within that medium.

Many studies have measured the relationship between radon concentration within a closed volume or radon flux density with atmospheric pressure. These studies have confirmed that as pressure falls, exhalation rate and concentration rise, and vice versa (Wilkening *et al.*, 1972; Wilkening and Hand, 1960; McLaughlin and Jonassen, 1980; Pohl-Ruling and Pohl, 1969). What is lacking in these studies, however, is an analytical and physical discussion of why the exhalation rate depends on pressure. The discussion below shows that flux density changes from soil were transient effects due to the rate of pressure variation. A more comprehensive discussion and summary may be found elsewhere (Hernandez, 1982).

The underground production rate of radon into the soil gas (emanation) is dependent only on soil properties (porosity, radium content, and moisture content) and not on atmospheric pressure and temperature (Tanner, 1980). Underground transport of the soil gas, which contains radon, occurs by bulk diffusion for typical soil properties (Wilkening, 1980).

In this transport regime, soil resistance to convective flow is quite large. Heat transfer occurs by conduction for the temperature gradients typically found underground, even for the large transient temperature gradients encountered near the soil surface (Paaswell, 1969). The reviews by Currie on the diffusion of gases in porous media (1960a; 1960b; 1961) show that the bulk diffusion coefficient is a very weak function of temperature, varying by 5% under most practical conditions. Regardless of the temperature condition, underground transport and exhalation of radon-containing soil gas is not temperature-induced.

Under steady atmospheric pressure, underground pressure gradients are zero and pressure-induced flow in a porous medium by Darcy's Law (permeation) is negligible. This conclusion is supported explicitly and implicitly by several analyses (Kraner *et al.*, 1963; Wilkening, 1980; Tanner, 1980; Colle *et al.*, 1981). The reviews by Currie also show that the diffusion coefficient in the bulk transport regime is a weak function of the steady value of underground pressure.

Only unsteady conditions of atmospheric pressure can induce changes in J_s. The magnitude of instantaneous J_s enhancement or suppression is dependent on the rate of pressure change and its duration. For a linear drop in pressure, the instantaneous value of $J_s(t)$ rises continuously until pressure variation ceases, as measured by Clements and Wilkening (1974), and can induce changes in J_s by a factor of 2. The relaxation time to steady underground pressure is on the order of several hours (Colle *et al.*, 1981).

Over periods of days pressure variation is oscillatory with a period on the order of 1 to several days, and an amplitude of 1%. In this case, $J_s(t)$ is alternatively enhanced and suppressed.

The average flux density under the periodic pressure is approximately equal to the flux density under steady pressure. For a sinusoidal oscillation, using the underground pressure model of Fukuda (1954), it can be shown that the Darcy velocity is sinusoidal in time (Hernandez, 1982). Edwards and Bates (1980) show analytically no net change in J_s over several periods for a periodic (square wave) pressure variation.

A porous medium, therefore, has a mean or "characteristic" value of J_s independent of atmospheric conditions of temperature and pressure. This value will change over periods as long as several months, while conditions of soil permeability (moisture content) and surface conditions (e.g., the presence of a snowpack) change. The characteristic value equals the instantaneous value only during times of steady atmospheric pressure.

Characteristic indoor radon source flux

The radon source flux into a chamber is the sum of the contributions from all the individual sources. Some of these will vary with time because of pressure variations or intermittent source terms (i.e., indoor water use with high radon concentration), but the magnitude of variation may be almost negligible. The portion of the source flux which originates in soil may be buffered by a

much less impermeable barrier, such as a poured concrete floor or finished wall, because the diffusion coefficients of radon in soil and concrete differ by about three orders of magnitude. Induced Darcy velocities in concrete will therefore be much smaller than in soil for similar pressure variations. If so, the time dependence of source flux with pressure will be reduced substantially (Hernandez, 1982).

In order to adjust for the possibility of changing source flux, however, barometric pressure should be monitored during experimental periods. Ideally, experiments should be performed on days of steady barometric pressure, with no water usage to reduce the time-dependence of source flux. Under these circumstances the results should yield a good value of the characteristic source flux.

Two-Chamber Model

According to Sinden (1978) buildings which cannot be modeled as a single, perfectly mixed chamber may be satisfactorily represented by a finite number of N chambers, each perfectly mixed, with positive volumetric air flows between the other $N - 1$ chambers and the outdoors. A multichamber system with $N = 4$ is shown in Fig. 1. Flows between chambers are called interchamber flows, while flows between a chamber and the outside are called infiltration flows.

For a tracer gas injection in one or more of the chambers under steady infiltration conditions and interchamber coupling, N eigenvalues and N eigenvectors, theoretically derivable from the tracer gas concentration decay plots in each chamber, completely determine the system flows. For an instantaneous injection in one or more of the chambers, the system solution is homogenous with N initial conditions.

The two-chamber system is much simpler, as shown in Fig. 2. The six volume flows are determined from the tracer gas balance:

$$\frac{dC_l}{dt} = -\frac{(F_{lb} + F_{lo})}{V_l} C_l + \frac{F_{bl}}{V_l} C_b, \tag{2a}$$

$$\frac{dC_b}{dt} = \frac{F_{lb}}{V_b} C_l - \frac{(F_{bl} + F_{bo})}{V_b} C_b, \tag{2b}$$

where subscripts b, l, and o denote the basement, living area, and outdoors, respectively. The complete solution for the two-chamber tracer gas concentrations with instantaneous injection is

$$\mathbf{C}(t) = \begin{bmatrix} C_l \\ C_b \end{bmatrix} = a_1 \xi_1 e^{\lambda_1 t} + a_2 \xi_2 e^{\lambda_2 t}. \tag{3}$$

Each eigenvalue λ_j is associated with an eigenvector ξ_j. The constants a_1 and a_2 account for initial conditions. The air change rates for the two chambers are defined by

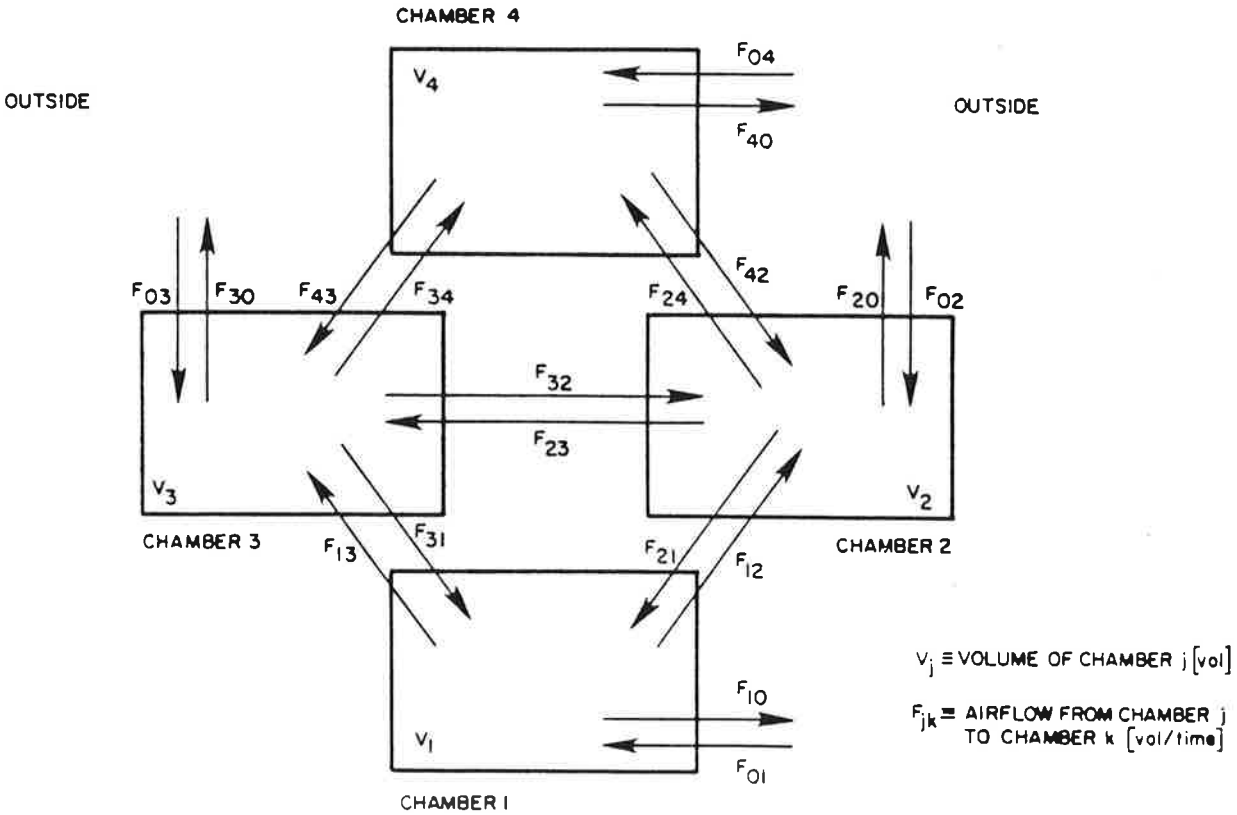

Fig. 1. Multichamber house model.

$F_{jk} \equiv$ INTERCHAMBER AIRFLOW FROM CHAMBER j TO CHAMBER k [vol/time]

$V_j \equiv$ VOLUME OF CHAMBER j [vol]

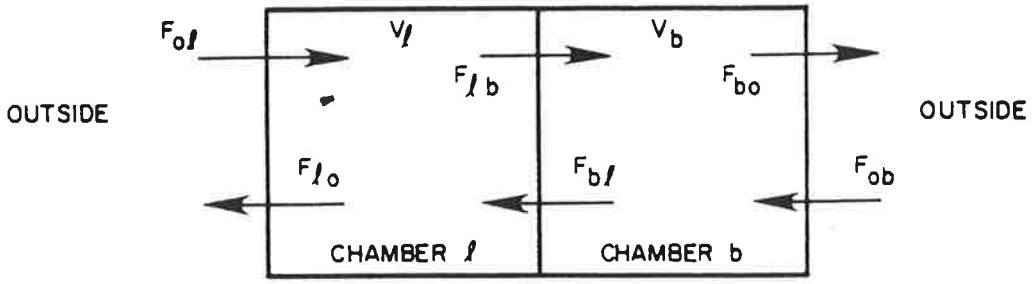

Fig. 2. Two-chamber flow model.

$$A_l = \frac{F_{bl} + F_{ol}}{V_l} = \frac{F_{lb} + F_{lo}}{V_l},$$

$$A_b = \frac{F_{lb} + F_{ob}}{V_b} = \frac{F_{bl} + F_{bo}}{V_b}.$$

By taking determinants the system eigenvalues and eigenvectors are found to be:

$$\lambda_{1,2} = -\tfrac{1}{2}(A_l + A_b) \pm \tfrac{1}{2}\left\{(A_l + A_b)^2 - 4\,\frac{F_{bl}F_{lb}}{V_b V_l}\right\}^{1/2}, \quad (4)$$

$$\xi_1 = \begin{Bmatrix} \dfrac{A_l + \lambda_1}{F_{bl}/V_l} \\ 1 \end{Bmatrix} = \begin{Bmatrix} \dfrac{F_{lb}/V_b}{A_b + \lambda_1} \\ 1 \end{Bmatrix}, \quad (5a)$$

$$\xi_2 = \begin{Bmatrix} \dfrac{A_l + \lambda_2}{F_{bl}/V_l} \\ 1 \end{Bmatrix} = \begin{Bmatrix} \dfrac{F_{lb}/V_b}{A_b + \lambda_2} \\ 1 \end{Bmatrix}. \quad (5b)$$

Two-chamber features

Figure 3A is a sample two-chamber tracer gas decay profile. The concentration decay in each chamber j is plotted as ln C_j vs time. The injected chamber concentration is designated $C_i(t)$ and the alternate chamber concentration is designated $C_a(t)$. The "injected" or "alternate" labels will be assigned to either the basement or living area as appropriate for a particular experiment and injection location.

The initial period of the second order profile is called the *transient* period because the relative tracer gas concentrations in the two chambers converge. Subsequently, during the *dominant* period, the two tracer gas concentrations both decay at the same log linear rate, with the ratio of their concentrations constant. The case shown in Fig. 3A is one of weak coupling, because the mixing of the tracer gas concentrations is not faster than the loss to the outside. $C_i > C_a$ over all time in this case.

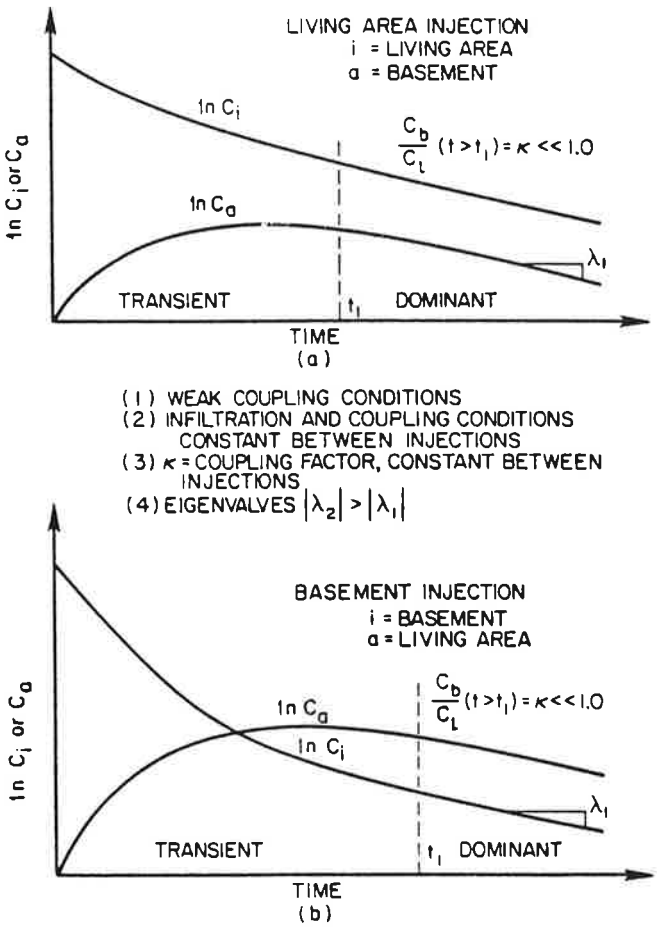

Fig. 3. Sample two-chamber tracer gas concentration profiles for injections in different chambers of the same house.

Be defining $|\lambda_2| > |\lambda_1|$ for two unequal eigenvalues the dominant period occurs after the transient term of

Eq. (3) dies out, for $t \gg (\lambda_2)^{-1}$. The dominant period tracer gas concentrations in both chambers are defined by $\mathbf{C}(t) = a_1\xi_1 e^{\lambda_1 t}$, with λ_1 as the log linear slope.

Alternatively, the concentration profile may resemble Fig. 3B. This is a case of concentration "crossover," where $C_i < C_a$ in the dominant region. Again, this is a weak coupling case because interchamber mixing is poor. The fact that the tracer gas concentrations are equal at one instant in time does not imply good mixing.

Under strong coupling the concentration profile will resemble Fig. 4. In this case we must have $|\lambda_2| \gg |\lambda_1|$. Interchamber mixing is fast, the transient period is relatively short, and $C_i = C_a$ in the dominant region.

If the two concentrations are roughly equal in the dominant period, interchamber mixing must be faster than the loss to the outdoors. The coupling factor $\varkappa$ is defined as the ratio of the smaller dominant eigenvector component to the larger. By this definition, $0 < \varkappa < 1.0$, with $\varkappa \sim 0$ indicating very weak coupling and $\varkappa \sim 1.0$ indicating very strong coupling.

The value of $\varkappa$ is not directly related to R_c. It can be shown, however, that weak coupling occurs for $\varkappa < 0.50$ and strong coupling occurs for $\varkappa > 0.85$, with intermediate values indicating moderate coupling (Hernandez, 1982).

Limiting cases

Using Eq. (4) it can be shown that as interchamber flows become very small, λ_1 and λ_2 approach A_i and A_b, the air change rates of the two chambers. At zero coupling, tracer gas concentrations would decay at distinct rates independent of the presence of the other chamber. Therefore, each chamber is "associated" with one of the eigenvalues.

As interchamber flows become very large, λ_2 becomes infinite. In the limit, mixing is instantaneous and λ_1 is the single decay rate for two perfectly coupled chambers (i.e., a single-chamber system).

An examination of the variation of eigenvalues with coupling, for constant infiltration flows, shows the functional relationship for λ_1, $\lambda_2 = f(\varkappa)$. Over the entire range of $\varkappa$ the larger of the two eigenvalues (λ_2) increases to infinity, but the smaller (λ_1) increases by only about 10%. Thus, a residence with variable coupling at steady infiltration conditions is described by a variable "mixing" eigenvalue [$\lambda_2 = f(\varkappa)$] and a roughly constant "infiltration" eigenvalue [$\lambda_1 \neq f(\varkappa)$] (Hernandez, 1982), both of whose lowest values are determined by the air change rates of the chambers under decoupled conditions.

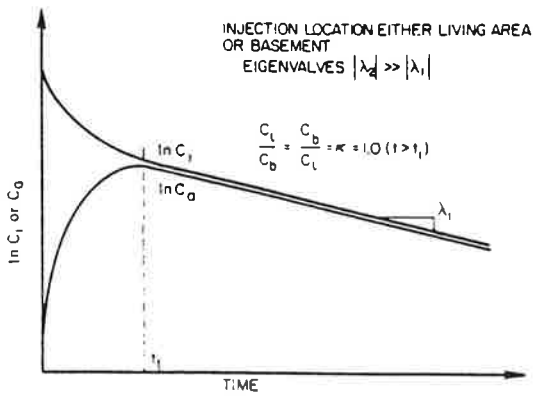

Fig. 4. Sample two-chamber tracer gas concentration profile for injection under strong coupling conditions.

Parameter invariability

In Eq. (3), constants a_1 and a_2 account for any initial conditions of tracer gas concentration. Therefore, the two eigenvalues and their associated eigenvectors, under any steady infiltration and coupling conditions, are *invariant*. Experimental measurement of these invariant parameters will be a suitable evaluation of the two-chamber model.

Figures 3A and 3B resemble the tracer gas concentration profiles for injections in different chambers of the same house under steady infiltration and coupling. In the dominant region, where $\mathbf{C}(t) = a_1\xi_1 e^{\lambda_1 t}$, it is immediately evident that the ratio of concentrations is invariant. The slope of the dominant region (λ_1) is also invariant. Transient parameters should also be invariant, but this would not be evident from the figures.

Parameter invariance means that an injection into one of the chambers of a weakly coupled system will produce a concentration crossover case. It can be shown analytically that this will occur for an injection into the chamber which is associated with the larger (transient) eigenvalue λ_2. This is because tracer gas loss to the outside is slower in the alternate chamber in this case.

Parameter and flow determination

For the two-chamber system, four of the six flows are independent and must be determined from the tracer gas decay data.

Equation (3) may be rewritten in the following form using the injected and alternate labels:

$$C_i(t) = a_{11}e^{\lambda_1 t} + a_{12}e^{\lambda_2 t}, \tag{6a}$$

$$C_a(t) = a_{21}e^{\lambda_1 t} + a_{22}e^{\lambda_2 t}. \tag{6b}$$

The constants a_{11}, a_{12}, a_{21}, and a_{22} all incorporate the initial conditions for a particular injection.

We define the eigenvector ratio as the ratio of the injected chamber component to the alternate chamber component of each eigenvector. Thus, relabeling Eqs. (5a) and (5b) we have

$$r_1 = \frac{a_{11}}{a_{21}} = \frac{A_i + \lambda_1}{F_{ai}/V_i} = \frac{F_{ia}/V_a}{A_a + \lambda_1}, \tag{7a}$$

$$r_2 = \frac{a_{12}}{a_{22}} = \frac{A_i + \lambda_2}{F_{ai}/V_i} = \frac{F_{ia}/V_a}{A_a + \lambda_2}. \tag{7b}$$

With this definition of r_1 and r_2, invariance across different injection locations requires that r_1 (living area) = $1/r_1$(basement) and r_2(living area) = $1/r_2$(basement).

Using Eqs. (7a) and (7b) the four linearly independent flows may be determined as a function of the values of r_1, r_2, λ_1, and λ_2. The other two flows are determined from air change rate balances. The results are shown below.

$$F_{ia} = V_a \frac{(\lambda_2 - \lambda_2)}{(r_2 - r_1)}, \tag{8a}$$

$$F_{al} = V_l \frac{(\lambda_2 - \lambda_1)}{\left(\frac{1}{r_2} - \frac{1}{r_1}\right)}, \tag{8b}$$

$$F_{oi} = V_i \left(\frac{\lambda_2 \left(\frac{1}{r_1} - 1\right) - \lambda_1 \left(\frac{1}{r_2} - 1\right)}{\left(\frac{1}{r_1} - \frac{1}{r_2}\right)} \right), \tag{8c}$$

$$F_{oa} = V_a \left(\frac{\lambda_2 (r_1 - 1) - \lambda_1 (r_2 - 1)}{(r_2 - r_1)} \right). \tag{8d}$$

The four system parameters, r_1, r_2, λ_1, and λ_2, must be determined from the tracer gas data. After the transient terms have died out, from Figs. 3A, 3B, and Eq. (6) it is evident that

$$\ln C_i = \ln a_{11} + \lambda_1 t, \tag{9a}$$

$$\ln C_a = \ln a_{21} + \lambda_1 t. \tag{9b}$$

Extrapolating the slope of λ_1 in the dominant region to $t = 0$ gives two intercepts, $\ln a_{11}$ and $\ln a_{21}$, for the injected and alternate chamber concentration profiles, respectively. Also, if $C_a(0) = 0$ then $a_{22} = -a_{21}$.

The transient parameters are similarly obtained after dominant parameter solution. Solving for the transient terms of Eq. (6) and taking logarithms we have

$$\ln[C_i - a_{11} e^{\lambda_1 t}] = \ln a_{12} + \lambda_2 t, \tag{10a}$$

$$\ln[a_{21} e^{\lambda_1 t} - C_a] = \ln(-a_{22}) + \lambda_2 t. \tag{10b}$$

A linear regression of the left-hand side of Eqs. (10) with time should yield two lines, both with slope λ_2 ($\lambda_2 < 0$, $|\lambda_2| > |\lambda_1|$) and with intercepts $\ln a_{12}$ and $\ln(-a_{22})$ in the injected and alternate chambers.

This procedure need not be used exclusively, especially when a concentration profile is not well-defined. Trial and error adjustments to the parameters may be necessary to fit data properly.

Radon source flux balance

Once the system flows are known, the steady radon source flux S_j (pCi/unit time) from all indoor sources in chamber j may be calculated using a radon flux balance, as shown in Fig. 5. Using the "injected" and "alternate" labels, the solutions are

$$S_i = (F_{io} + F_{ia} + \lambda_{Rn} V_i) I_i - F_{oi} I_o - F_{ai} I_a, \tag{11a}$$

$$S_a = (F_{ao} + F_{ai} + \lambda_{Rn} V_a) I_a - F_{oa} I_o - F_{ia} I_i. \tag{11b}$$

The terms $F_{ia} I_i$ and $F_{ai} I_a$ are the convective interchamber radon fluxes of the system. Their magnitude relative to convective infiltration radon fluxes figure prominently in the source flux error described below.

Source flux error δS_j is determined using the root/sum/square method. For $y = f(x_1, x_2 \ldots x_n)$ the probable error δy for standard deviation δx is

$$\delta y = \left\{ \sum_{k=1}^{n} \left(\frac{\partial y}{\partial x_k} \delta x_k \right)^2 \right\}^{1/2} \tag{12}$$

Parameter error affects system flows as δF, and statistical counting error in radon measurement is δI.

Experiment Description and Procedure

Nine two-chamber tracer gas injections in three Princeton, NJ, homes were performed during spring and summer 1981. Within each house, parameter invariability was examined across different initial conditions and in one residence (LL) source flux results were compared across different infiltration and coupling conditions.

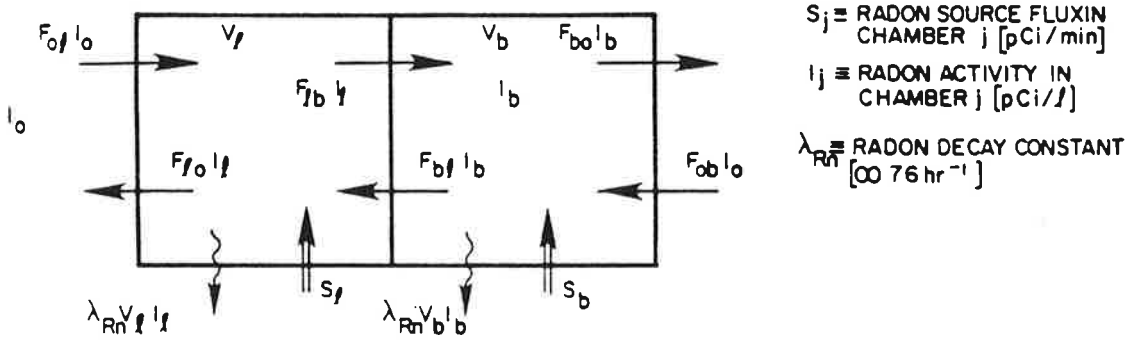

Fig. 5. Two-chamber radon flux balance.

To test parameter invariability, injections were performed in pairs, one each in living area and basement, on a day deliberately chosen for calm weather. For one night prior to each experiment, house occupants were asked to keep windows and doors closed except for entry to assure minimal perturbation of the steady radon concentrations. It was assumed that infiltration conditions were constant during the day that a pair of injections was performed.

Experiments in the LL house were conducted as following: experiments in different seasons provided variable infiltration, experiments by injection pair provided variable initial conditions, and experiments on consecutive days with the indoor air circulation fan on or off provided variable coupling under constant infiltration conditions.

The tracer gas used was sulfur hexafluoride. It was injected manually and mixed by handheld fans throughout the injected chamber. Tracer gas was monitored alternately in both chambers every 2 min by the Automated Air Infiltration Unit (AAIU) (Harrje *et al.*, 1974) developed jointly by Princeton and the National Bureau of Standards. The AAIU detects tracer gas using electron capture detectors in combination with a gas chromatograph.

Air samples were measured for their radon content using the Princeton-built radon scintillation counter (RASC). The RASC consists of an EMI Gencom photomultiplier tube, a linear amplifier and discriminator, and a scalar. It counts the alpha scintillations produced by alpha particle interaction with a phosphor-coated commercial scintillation flask.

Experimental Results

Table 3 shows the injection condition summaries, parameter comparisons, and source flux calculations and errors by residence and by injection pair for nine experiments. Atmospheric pressure trends during each experiment are noted as either steady or by some linear rate of change.

All four two-chamber system parameters are compared by injection pair to test parameter invariability. Living area and basement source fluxes are compared across all experiments in a particular residence to test the characteristic source flux concept.

Table 4 shows the six system flows calculated from the experimental data. It permits comparison of system eigenvalues and chamber air change rates between themselves and as a function of coupling.

Two chamber model discussion

Tracer gas concentration profiles. The experimental data for nine tracer gas experiments are shown in Figs. 6–14. In general, they demonstrate that houses behave as two-chamber systems. Each experiment produced a two chamber decay profile except for LL-TG-1, R-TG-2, and T-TG-3. The first two of these, however, occurred under such weak coupling that tracer gas concentration decay was log linear in the injected chamber and almost undetectable in the alternate chamber. In T-TG-3 the alternate chamber profile had a slight inflection, indicating that either the system order was greater than 2 or, more likely, that infiltration or coupling was not constant throughout the experiment. The weak coupling cases do not undermine the two-chamber hypothesis but demonstrate one of the limiting processes in interchamber coupling.

In these figures, tracer gas profiles are compared with the curves described by the derived parameters. Comparison is good in all cases, except for T-TG-3 due to its irregular profile. Parameter determination for this experiment required some trial and error, as it did for experiment LL-TG-4.

Table 4. System flow and air change rate summary for nine two-chamber tracer gas experiments.

Injection	Infiltration Flows (l/min)				Interchamber Flows (l/min)		Chamber Air Change Rate (h^{-1})		Eigenvalues (h^{-1})		Coupling Factor[a]
	F_{ia}	F_{oi}	F_{ba}	F_{ob}	F_{ib}	F_{bi}	A_i	A_b	λ_1	λ_2	κ
LL-TG-1[b]	–	–	1734	1734	–	–	–	0.51	–	0.51	–
LL-TG-2	841	534	860	1167	283	590	0.26	0.43	0.21	0.48	0.38
LL-TG-3	2053	2609	1080	524	832	276	0.62	0.35	0.31	0.66	0.19
LL-TG-4[c]	431	1227	1713	911	1111	315	0.33	0.53	0.29	0.60	(weak)[d]
LL-TG-6[e]	337	1372	2162	1127	5026	3991	1.15	1.61	0.29	2.46	1.0
T-TG-3[c,e]	2	1526	3814	1290	4230	2706	0.85	1.96	0.41	2.40	0.81
T-TG-4[e]	1993	1294	1120	1819	3074	3773	1.01	1.47	0.37	2.1	0.85
R-TG-1[c]	653	637	1399	1415	120	136	0.15	0.69	0.15	0.69	0.10
R-TG-2[b]	–	–	1380	1380	–	–	–	0.62	–	0.62	–

[a]Coupling factor has bounds $0 < \kappa < 1$, where $\kappa \to 0$ implies weak coupling and $\kappa \to 1.0$ implies strong coupling.
[b]Very weak coupling; alternate chamber tracer gas signal either below AAIU threshold or not monitored. $\kappa \sim 0$.
[c]Some or all parameters obtained by trial and error.
[d]Estimated coupling factor (by curvature extrapolation) indicated strong coupling but other coupling criteria (including $\lambda_1 \sim A_i$, $\lambda_2 \sim A_b$) indicated weak coupling.
[e]Strong coupling deliberately induced by turning on indoor air circulation fan.

Table 3. Experimental summary for nine two-chamber tracer gas experiments.

Experiment	Date	Injection Location[a]	Pressure Trend (mbar/h)	Radon Concentration[b] I_i (pCi/l)	I_b	Eigenvalues λ_1 (min^{-1})	λ_2	Eigenvector Ratio[c] r'_1	r'_2	Coupling χ	Source Flux S_i(pCi/min)	S_b	Source Flux Ratio θ	Error $\frac{\delta S_i}{S_i}$	$\frac{\delta S_b}{S_b}$
LL House (V_b = 230,000 l; V_i = 280,000 l)															
LL-TG-1	4/10/81	B	rising, +0.75	1.6	6.5	–	−0.0085	–	–	0[e]	–	11,960	–	–	0.16
LL-TG-2	4/10/81	LA	falling, −0.50	1.6	6.5	−0.0035	−0.0080	2.6	−0.43	0.38	−1100	9410	0.0	1.0[d]	0.16
LL-TG-3	8/18/81	B	steady	2.7	7.5	−0.0052	−0.011	0.19	−1.41	0.19	5500	8100	0.56	0.22	0.20
LL-TG-4	8/18/81	LA	steady	2.5	5.4	−0.0049[f]	−0.010[f]	0.91[f]	−0.25[f]	(weak)[g]	2000	9100	0.18	0.28	0.19
LL-TG-6	8/19/81	LA	steady	4.9	5.9	−0.0049	−0.041	1.0	−0.65	1.0	2770	11,730	0.20	1.86	0.50
T House (V_b = 200,000 l; V_i = 300,000 l)															
T-TG-3	4/29/81	B	falling, −0.37	7.4	8.3	−0.0068	−0.040[f]	1.23	−0.34[f]	0.81	8710	23,440	0.25	0.66	0.39
T-TG-4	4/29/81	LA	briefly falling, then rising, +0.78	7.4	8.3	−0.0062	−0.035	1.18	−0.69	0.85	5950	18,400	0.21	1.21	0.37
R House (V_b = 134,000 l; V_i = 300,000 l)															
R-TG-1	5/11/81	LA	falling, −0.45	1.4	10.5	−0.0025	−0.0115[f]	10.0	−0.05	0.10	−300	15,900	0.0	4.33[d]	0.16
R-TG-2	5/21/81	B	falling, −0.16	–	4.4	–	−0.0105	–	–	0[e]	–	6020	–	–	0.12

[a]LA = living area; B = basement.
[b]Average of more than one air sample.
[c]Eigenvector ratios redefined as the ratio of the living area eigenvector component to the basement component. For a living area injection, $r' = r$, and for a basement injection, $r' = 1/r$.
[d]Source flux error includes parameter error.
[e]Coupling very weak; alternate chamber tracer gas concentration either below AAIU threshold or not monitored.
[f]Parameter obtained by trial-and-error fit to data.
[g]The estimated coupling factor (obtained by curvature extrapolation) indicated strong coupling but all other coupling criteria indicated weak.

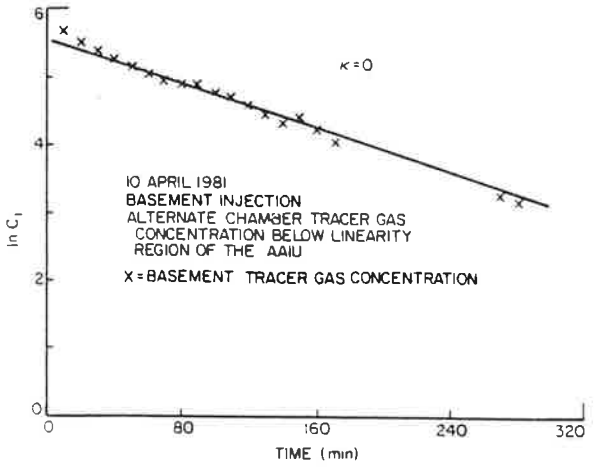

Fig. 6. Tracer gas experiment LL-TG-1.

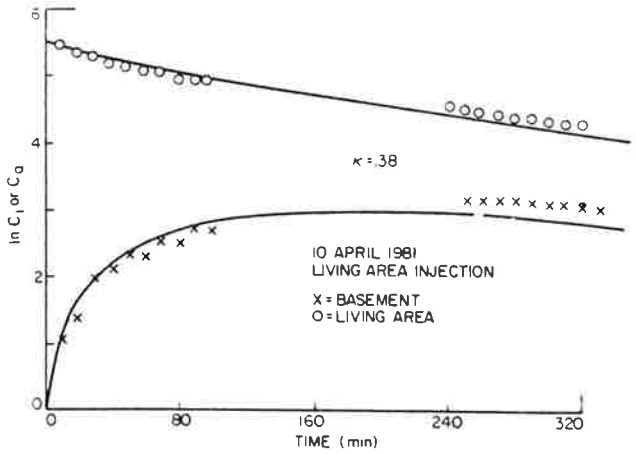

Fig. 7. Tracer gas experiment LL-TG-2.

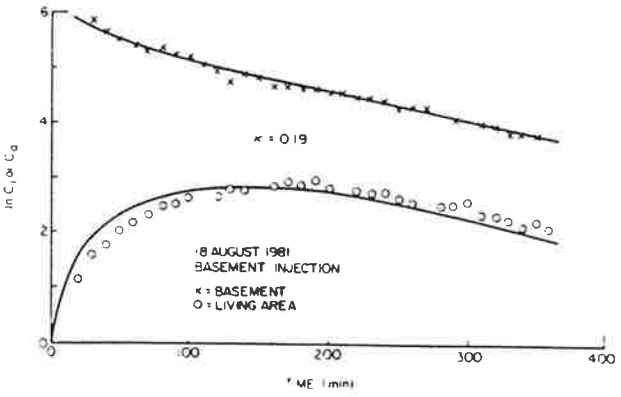

Fig. 8. Tracer gas experiment LL-TG-3.

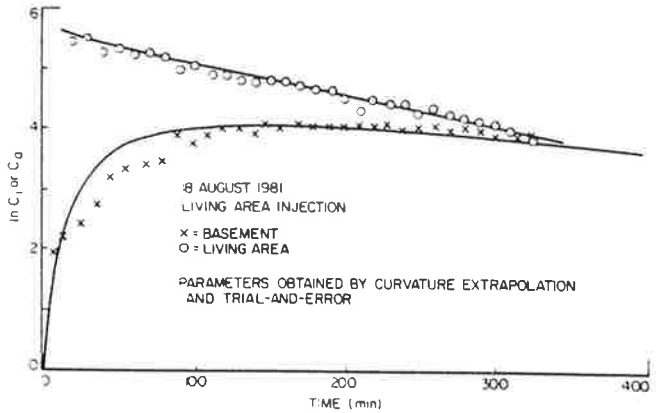

Fig. 9. Tracer gas experiment LL-TG-4.

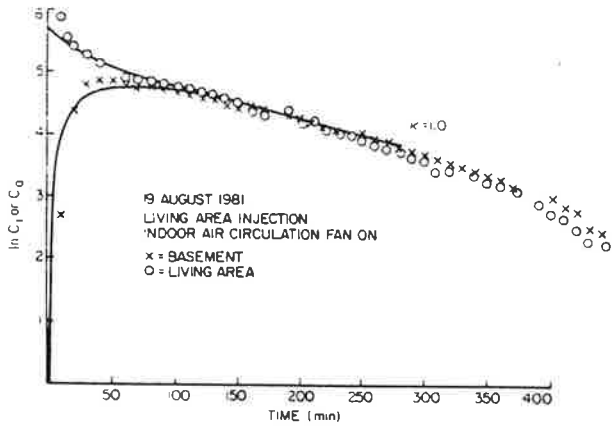

Fig. 10. Tracer gas experiment LL-TG-6.

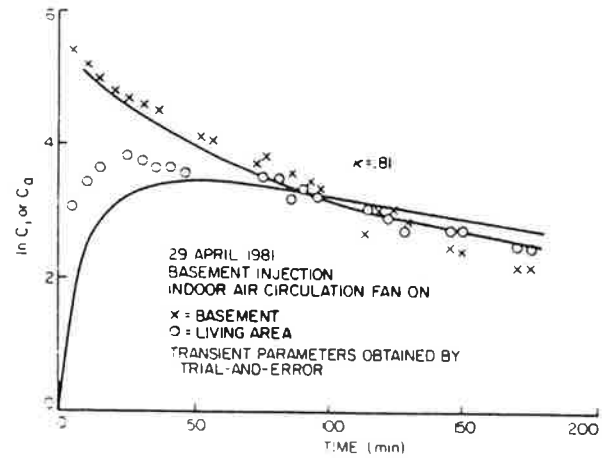

Fig. 11. Tracer gas experiment T-TG-3.

Interchamber coupling. For the experiments in the LL and T houses, strong coupling ($\varkappa > 0.85$) was encountered only when the air circulation fan was on, as indicated in Table 4. When the fan was off, coupling was weak, with $\varkappa < 0.40$. For strong coupling, Table 4 shows that the magnitude of the interchamber flows are greater than the magnitude of the infiltration flows. This is an internal consistency which supports the two-chamber model.

Parameter error. System eigenvalues obtained by linear regression in nearly all cases had high correlation coefficients ($r^2 > 0.85$). Only one of the four eigenvector co-

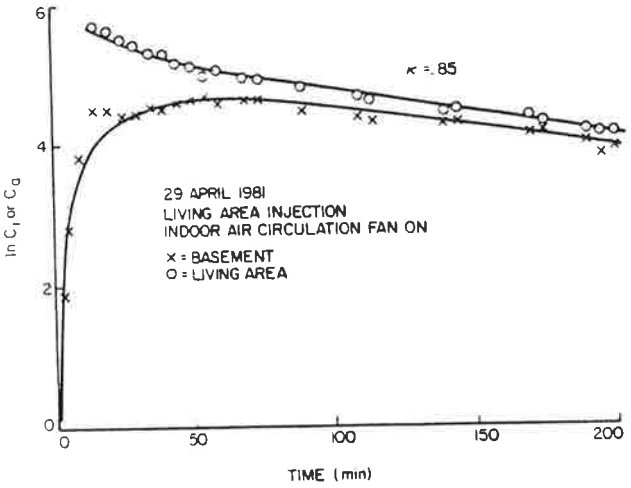

Fig. 12. Tracer gas experiment T-TG-4.

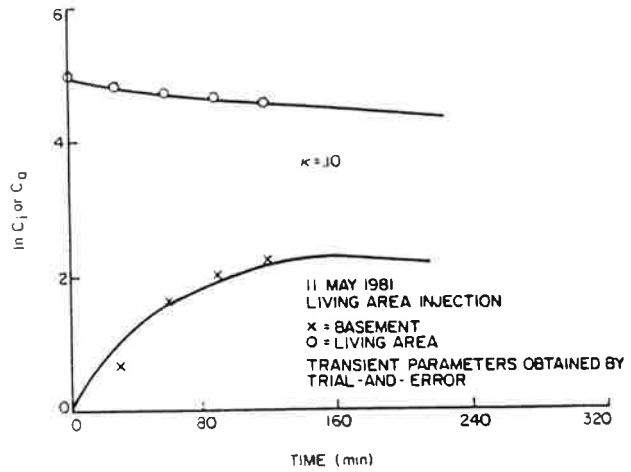

Fig. 13. Tracer gas experiment R-TG-1.

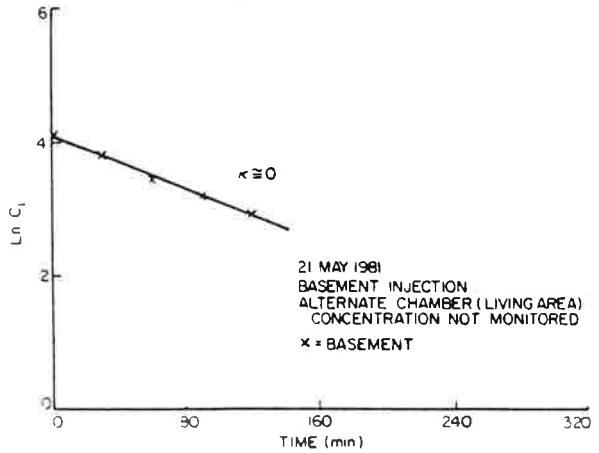

Fig. 14. Tracer gas experiment R-TG-2.

efficients, a_{12}, was not always determined reliably, primarily due to scatter in the injected chamber tracer gas concentration near injection time.

System parameters, flows, and invariance. Parameter comparisons are made in Table 3. Note that the redefined eigenvector ratios r'_1 and r'_2 facilitate comparison.

In all four injection pairs eigenvalue comparisons were excellent under strong and weak coupling conditions. In the weak coupling cases, LL-TG-1 and R-TG-2, only one decay mode was evident but it was equal to one of the decay modes found in its associated injection.

Eigenvector comparisons were not as successful. The two cases of extremely weak coupling precluded determination of any eigenvectors; in both of the other two injection pairs (T-TG-3 and 4, LL-TG-3 and 4) irregularities in both crossover case experiments required trial and error fit of some parameters to tracer gas data.

Some useful conclusions may still be drawn. Despite the irregularity of T-TG-3, the injection pair still demonstrated dominant eigenvector invariability, with only a 7% difference, as evident from Figs. 11 and 12. The transient eigenvectors differed by a factor of 2, but these values were obtained by trial and error, reducing confidence in the comparison.

The presence of the "infiltration" and "mixing" eigenvalues was detected in experiments LL-TG-3, 4, and 6. Experimental data from the three injections, which were made on consecutive days during stable, mild summer weather, displayed the same dominant eigenvalue (about 0.0050 min^{-1}, see Figs. 8–10) though the coupling difference was dramatic ($x = 0.19$ vs $x = 1.0$).

The result is interesting. The functional relationship of the two eigenvalues with coupling was determined assuming constant infiltration flows and variable interchamber flows. From Table 4, it is evident that the derived infiltration flows were anything but constant across the three experiments. One explanation is that the (steady) infiltration eigenvalue detected is experimental data, while the system flows are calculated quantities from algebraic combinations of four derived parameters. The calculated quantities would incorporate considerably more uncertainty as a result.

From Table 4 it can also be seen that for the weak coupling cases the system eigenvalues are approximately equal to the chamber air change rates. Under strong coupling, the opposite conclusion can be drawn. This result is again consistent with the analytical development of a two-chamber model.

Concentration crossover. The concentration crossover case was detected twice in experiments LL-TG-4 and T-TG-3. In these cases, the transient region was much more long-lived than in the other experiment of the injection pair, necessarily making data monitoring longer (for LL-TG-4, monitoring ceased before the transient region in the alternate chamber ended). This decreases the likelihood of steady conditions throughout the experiment. It is recommended that injection locations be

chosen in the chamber associated with the smaller air change rate to avoid the crossover case.

Source flux comparisons

The good comparison between basement source flux results basically confirmed the presence of the characteristic source flux. Source flux invariability was shown to exist across different infiltration, coupling, and injection conditions in one house. Comparisons for each house are discussed below.

The two mean basement source fluxes calculated from the T house injections varied by 8% from their average. The five mean basement flux results in the LL house varied by 17% from the average mean value of about 10,000 pCi/min. This good comparison spanned variations in coupling, infiltration, and initial conditions.

Only in the R houses did the basement flux results differ substantially, by a factor of 2.5. The large discrepancy between the two results may be explained by the pressure trends. The larger source flux result (R-TG-1) was obtained while the barometric pressure was falling at a rate three times higher than the rate during the other experiment (R-TG-2). Though similar rates were encountered during experiments in other houses, the R-house basement surface, which consists of crumbling finishing and occasional soil exposure, may provide a poorer diffusion barrier than the poured concrete and cinderblock surfaces of the LL and T house.

This conclusion is supported by the more than 15-fold variation in R-house basement radon concentration for 12 samples taken between April and June 1981. During this period, highest concentrations occurred during periods of falling pressure and lowest concentrations during rising pressure. The same relation could not be detected for the other two houses (Hernandez *et al.*, 1982).

Source flux error. Statistical error in radon counting accounted for the major fraction, if not all, of the source flux error. Only in two cases did system parameter error significantly increase the error result, as noted in Table 3.

In any two-chamber system source flux error will depend upon two factors: the magnitude of interchamber coupling and the relative magnitude of the source flux in the *other* chamber (Hernandez, 1982). Highest source flux error (by percent) would occur in the living area of a house with a zero source flux ratio [$\theta = (S_l/V_l)/(S_b/V_b)$] and under strong coupling. Both the larger basement source flux and the large interchamber flows produce a large convective radon flux from the basement to the living area with its associated error.

These trends may be seen in Table 3. Percent error is greater in the chamber with the smaller source flux (the living area), and error increases with increasing coupling at a constant ratio between source fluxes. Basement source fluxes were in all cases much greater than living area fluxes, and most cases δS_l was a large fraction of S_l. As a result, S_l comparison within a residence was not successful.

Unquantifiable errors may also account for the source flux variations between experiments in a house. Unsteady conditions of radon exhalation, system flows, or radon concentrations would affect the steady balances of Eq. (11). Changing infiltration rate during an experiment is evident in experiment LL-TG-6 (Fig. 10), where past $t = 340$ min the rate doubles from its previous value. Changing volume flows may account for the irregular profile of T-TG-3.

One-chamber vs two-chamber comparisons. The one- and two-chamber source flux models were compared by fitting both models to the seven sets of tracer gas experimental data with two-chamber profiles. Typically, one-chamber models utilize simultaneous measurement of only the living area radon concentration and log linear tracer gas decay rate. It assumes that the living area is completely decoupled from any other indoor volume. In the comparison of the seven experiments, the one-chamber model is fit to tracer gas data in the injected chamber of the two-chamber experiment. A log linear line is fit to about five data points (at approximately 30, 60, 90, 120, and 180 min). The comparisons are shown in Table 5.

In the three houses tested, most of the indoor source flux occurs in the basement, so the one-chamber basement injection results are comparable to the two-chamber results under moderate to weak coupling. The one-chamber living area comparisons show an underestimate of 60%–90% under weak coupling and 30%–50% under strong coupling.

What is even more dramatic is the variation in apparent flux result as a function of coupling in the LL house. Across the three living area injections (LL-TG-2, 4, and 6) the one-chamber result varies by a factor of 6 compared with the two-chamber variation of a factor of 1.5.

In general, any one-chamber experiment in a strongly coupled system, regardless of source flux location, will underestimate the source flux by an amount proportional to the fraction of indoor volume which is assumed to be decoupled from the experimental volume. Under weak coupling, the magnitude of underestimate will be qualitatively the same as the results of Table 5 if most of the source flux occurs in the basement.

Conclusions

The indoor radon source flux may be badly underestimated if a one-chamber model is applied to the living area volume only. The apparent source flux in this case is the combination of the actual living area source flux, if any, and the convective radon flux from the basement. The convective flux is only a fraction of the basement source flux (depending upon coupling); thus, the model cannot accurately determine the source flux if it

Table 5. Radon source flux comparisons between one- and two-chamber models.

	Injection	Coupling Factor, x	Total Indoor Source Flux (pCi/min) One-Chamber Model	Two-Chamber Model	One-Chamber Underestimate (%)
Basement Injection	LL-TG-3	0.19	14,000	13,600	0
	T-TG-3	0.81	27,770	32,100	13
Living Area Injection	LL-TG-2	0.38 (weak)[a]	1320	9410	86
	LL-TG-4		4200	11,100	62
	LL-TG-6	1.00	7540	14,500	48
	T-TG-4	0.85	16,880	24,300	31
	R-TG-1	0.10	1430	15,900	91

[a]Coupling factor for this injection indicated strong coupling but all other coupling criteria indicated weak.

is primarily located in the basement. Some of the variations in indoor source fluxes reported to date may be due to coupling changes over time within a residence. If coupling extremes between the basement and living area can be obtained the one-chamber model will more accurately measure the source flux into the chamber from building materials or the geologic substrate.

Acknowledgements—The authors thank Professor Robert Socolow for his project support and Professor Harvey Sachs for his critical analysis and boundless enthusiasm.

This work was supported by the United States Department of Energy contract No. DE-AC02-77CS20062 and was assisted by the National Science Foundation graduate fellowship program.

References

American Society of Heating, Refrigerating, and Air-Conditioning Engineers (1977), *ASHRAE Handbook and Product Directory 1977 Fundamentals*. ASHRAE, Inc., New York, NY.

Bonne, U., Patani, A., Leslie, C. M., DeWerth, D. W. (1979) Dynamic computer and laboratory simulations of gas-fired central heating systems. International Symposium on Simulation Modeling and Decision in Energy Systems, 19–21 June 1979, Montreux, Switzerland.

Clements, W. E. and Wilkening, M. H. (1974). Atmospheric pressure effects on the Rn-222 transport across the earth-air interface, *J. Geo. Res.* 79, 5025–5029.

Colle, R., Rubin, R. J., Knab, L. I., and Hutchinson, J. M. R. (1981) Radon transport through and exhalation from building materials. Technical Note 1139, National Bureau of Standards, Washington, DC.

Currie, J. A. (1960a) Gaseous diffusion in porous media. Part 1. A non-steady state method, *Brit. J. App. Phys.* 11, 314–317.

Currie, J. A. (1960b) Gaseous diffusion in porous media. Part 2. Dry granular materials, *Brit. J. App. Phys.* 11, 318–324.

Currie, J. A. (1961) Gaseous diffusion in porous media. Part 3. Wet granular materials, *Brit. J. App. Phys.* 12, 275–281.

Edwards, J. C. and Bates, R. C. (1979) Theoretical evaluation of radon emanation under a variety of conditions, *Health Phys.* 39, 263–274.

Fukuda, A. (1955) Air and vapor movement in soil due to wind gustiness, *Soil Sci.* 79, 249–258.

George, A. G. and Breslin, A. J. (1980) The distribution of ambient radon and radon daughters in residential buildings in the New York–New Jersey area, in *Natural Radiation Environment III*, T. F. Gesell and W. M. Lowder, eds. CONF-780422, National Technical Information Service, U.S. Department of Commerce, Springfield, VA.

Harrje, D. T., Hunt, C. M., Treado, S. J., and Malek, N. J. (1975) Automated instrumentation for air infiltration measurements in buildings. Report No. 13, Center for Environmental Studies, Princeton University, Princeton, NJ.

Hernandez, T. L. (1982) Radon source flux measurement in residences using a two-chamber ventilation model. M.S. (Engineering) thesis, PU/CEES-133, Center for Energy and Environmental Studies, Princeton University, Princeton, NJ.

Hernandez, T. L., Ring, J. W. and Sachs, H. M. (1982) The variation of basement radon concentration with barometric pressure or the curious case of the breathing basement. PU/CEES-144, Center for Energy and Environmental Studies, Princeton University, Princeton, NJ.

Kraner, H. W., Schroeder G. L., and Evans, R. D. (1963) Measurements of the effects of atmospheric variables on radon-222 flux and soil gas concentrations, in *The Natural Radiation Environment*, J. A. S. Adams and W. M. Lowder, eds. The University of Chicago Press, Chicago, IL.

McLaughlin, J. P. and Jonassen, N. (1980) The effects of pressure drops on radon exhalation from walls, in *Natural Radiation Environment III*, T. F. Gesell and W. M. Lowder, eds. CONF-780422, National Technical Information Service, U.S. Department of Commerce, Springfield, VA.

Paaswell, R. E. (1969) Transient temperature influences on soil behavior, in Effects of temperature and heat on the engineering behavior of soils, proceedings of an International Conference, 16 January, 1981. Sponsored by the Highway Research Board, Publication 1641, National Academy of Sciences, Washington, DC.

Pohl-Ruling, J. and Pohl, E. (1969) The radon-222 concentration in the atmospheres of mines as a function of the barometric pressure, *Health Phys.* 16, 579–584.

Sachs, H. M., Hernandez, T. L. and Ring, J. W. (1982) Regional geology and radon variability in buildings. *Environ. Int.* 8, 97–103.

Sinden, F. (1978) Theory of multichamber air infiltration, *Build. Environ.* 13, 21–28.

Tanner, A. B. (1980) Randon migration in the ground: A supplementary review, in *Natural Radiation Environment III*, T. F. Gesell and W. M. Lowder, eds. CONF-780422, National Technical Information Service, U.S Department of Commerce, Springfield, VA.

Wilkening, M. H. and Hand, J. E. (1960) Radon flux at the earth-air interface, *J. Geo. Res.* 65, 3367–3370.

Wilkening, M. H., Clements, W. E., and Stanley, D. (1972) Radon-222 flux measurement in widely separated regions, in *The Natural Radiation Environment II*, J. A. S. Adams, W. M. Lowder, and T. F. Gesell, eds. CONF-720805-PL, National Technical Information Service, U.S. Department of Commerce, Springfield, VA.

Wilkening, M. H. (1980) Radon Transport Processes Below the Earth's Surface, in *Natural Radiation Environment III*, T. F. Gesell and W. M. Lowder, eds. CONF-780422, National Technical Information Service, U.S. Department of Commerce, Springfield, VA.